© SEP 2026 | IRE Journals | Volume 10 Issue 3 | ISSN: 2456-8880
DOI: https://doi.org/10.64388/IREV10I3-1722903

CFD Based Analysis on Effect of Heat Transfer and Pressure Drop on Solar Air Heater

CH. BHANUSRI[1], K. MEGHANA[2]
[1]*Assistant Professor, Department of Mechanical Engineering, Sanketika Vidya Parishad Engineering College, Visakhapatnam.*
[2]*PG Scholar, Department of Mechanical Engineering, Sanketika Vidya Parishad Engineering College, Visakhapatnam.*

Abstract- Solar air heaters (SAHs) are attractive for low- and moderate-temperature thermal applications, but conventional smooth absorber plates provide limited heat transfer because of the viscous sub-layer near the heated surface. The present work investigates the thermo-hydraulic performance of a rectangular solar air heater using V+arc and Multiple V+arc artificial roughness geometries. Three-dimensional CFD simulations were performed in ANSYS Fluent 2024 R1 using the SST k–ω turbulence model for Reynolds numbers from 3000 to 11,000 under a uniform heat flux of 1000 W/m². The computational duct has a width of 100 mm, height of 20 mm, test length of 600 mm, roughness pitch of 20 mm, roughness height of 2 mm, and aspect ratio of 5. Experimental measurements were also conducted using an aluminium absorber plate, PT-100 temperature sensors, an anemometer, pyranometer, data logger and U-tube manometer. The Multiple V+arc configuration produced the highest heat-transfer enhancement, with Nusselt number increasing from 37.67 at Re = 3000 to 108.93 at Re = 11,000, approximately 2.9–3.1 times the smooth-plate baseline. The friction factor increased because of flow separation and secondary vortices, with values of approximately 0.030–0.027 for Multiple V+arc. The maximum thermo-hydraulic performance parameter of 2.057 was obtained at Re = 7000. Smooth-plate experimental results showed close agreement with the Dittus–Boelter and Blasius correlations, and the CFD results showed good agreement with experiment. The study demonstrates that Multiple V+arc roughness can substantially improve heat transfer while maintaining a favorable overall thermo-hydraulic performance.

Keywords—solar air heater, artificial roughness, V+arc, Multiple V+arc, CFD, Nusselt number, friction factor, thermo-hydraulic performance.

I. INTRODUCTION

The increasing demand for clean and renewable energy has intensified interest in solar thermal technologies. Solar energy can be converted directly into electricity through photovoltaic systems or into useful heat through solar thermal collectors. Solar air heaters are simple solar thermal devices in which an absorber surface captures incident radiation and transfers the resulting heat to air flowing through a duct. Their low operating cost, simple construction and applicability to drying and space-heating duties make them attractive for low- to moderate-temperature applications.

A major limitation of a conventional smooth-plate solar air heater is the relatively low convective heat-transfer coefficient of air. A viscous sub-layer forms close to the heated absorber surface and behaves as an additional thermal resistance. Artificial roughness elements can disturb this sub-layer, promote turbulence, generate secondary flow and improve mixing between the core air and the near-wall region. However, the same roughness also increases flow resistance, pressure drop and the power required to drive the air.

A number of roughness arrangements have therefore been investigated, including transverse ribs, inclined ribs, V-shaped ribs, multiple V-ribs, broken ribs, arc-shaped ribs and protrusions. Previous studies reported that rib height, pitch, relative roughness height, relative roughness pitch, aspect ratio and angle of attack strongly affect the resulting heat-transfer and friction characteristics [1]–[8]. Studies on multiple arcs, V-ribs and hybrid rib arrangements further show that secondary vortices can provide large thermal enhancement, although the hydraulic penalty must be considered simultaneously [9]–[15].

The present study focuses on a combined V+arc artificial roughness and a Multiple V+arc arrangement. The investigation combines three-dimensional CFD with experimental measurements and uses a smooth absorber plate as the baseline for validation. The principal objective is to determine how the roughness geometries influence temperature distribution, velocity field, pressure drop, Nusselt number, friction factor and thermo-hydraulic performance over Re = 3000–11,000.

Research gap and objectives

The literature reviewed in the project indicates that artificial roughness generally improves heat transfer but increases frictional losses. The present work addresses the need to examine the coupled thermal and hydraulic behavior of V+arc and Multiple V+arc configurations using a common duct geometry and a combined CFD–experimental approach. The objectives are: (i) develop three-dimensional CFD models for a smooth plate, V+arc and Multiple V+arc absorber surfaces; (ii) identify a suitable turbulence model; (iii) evaluate heat transfer and pressure-drop characteristics over the selected Reynolds-number range; (iv) fabricate and test an experimental setup using the same principal parameters; and (v) compare the computational and experimental smooth-plate results for validation.

II. LITERATURE REVIEW

Jain et al. investigated arc-shaped ribs with multiple gaps and reported improved thermo-hydraulic behavior associated with secondary flow and vortex formation [1]. Mahanand and Senapati studied quarter-circular ribs and found that the geometry enhanced fluid mixing and convective heat transfer [2]. Thakur examined multi-staggered W-shaped roughness and emphasized the trade-off between thermal enhancement and friction loss [3]. Reviews by Singh and Narayanan, Kabeel et al., Singh and Singh, and Alam and Kim summarize the broad use of artificial roughness and identify geometry optimization and CFD validation as important areas for further development [4], [16]–[18]. Yadav and Bhagoria reported the effectiveness of equilateral triangular ribs in CFD-based solar-air-heater analysis [6], while Kumar et al. and Hans et al. developed correlations for multi-V rib arrangements [7], [8]. Khanlari et al. examined perforated baffles, and Afshari et al. investigated turbulator modifications [9], [10]. Karmare and Tikekar, Bhattacharyya et al., and Pandey and Bajpai further demonstrated that different roughness configurations can substantially enhance heat transfer but may increase pressure losses [11]–[13]. Gawande et al. combined experimental and CFD methods for chamfered square ribs, reinforcing the value of numerical validation against experimental data [14]. Promvonge and Skullong and Nidhul et al. investigated hybrid and ribbed configurations for enhanced heat transfer and drying applications [19], [20].

Overall, the reviewed work shows that increasing Reynolds number generally raises Nusselt number while friction factor decreases. At the same time, the addition of artificial roughness increases friction relative to a smooth duct. This establishes the need for a performance parameter that balances thermal enhancement against hydraulic penalty. The present work uses the thermo-hydraulic performance parameter together with experimental and CFD validation.

III. COMPUTATIONAL METHODOLOGY

A. Computational domain and geometry

A three-dimensional rectangular solar air heater duct containing entrance, test and exit sections was modeled. The entrance section is 350 mm, the test section is 600 mm and the exit section is 200 mm. The duct width is 100 mm and height is 20 mm, giving an aspect ratio W/H = 5. The artificial roughness has a pitch P = 20 mm and height e = 2 mm, corresponding to P/e = 10. For the Multiple V+arc configuration, the project uses a relative roughness width of 6 and an attack angle of 60°. A uniform heat flux of 1000 W/m² is applied to the absorber plate.

© SEP 2026 | IRE Journals | Volume 10 Issue 3 | ISSN: 2456-8880
DOI: https://doi.org/10.64388/IREV10I3-1722903

Parameter	Value
Entrance length, L_1	350 mm
Test length, L_2	600 mm
Exit length, L_3	200 mm
Duct width, W	100 mm
Duct height, H	20 mm
Roughness pitch, P	20 mm
Roughness height, e	2 mm
Relative pitch, P/e	10
Aspect ratio, W/H	5
Heat flux	1000 W/m²
Reynolds number	3000–11000

Table 1. Geometrical and operating parameters.

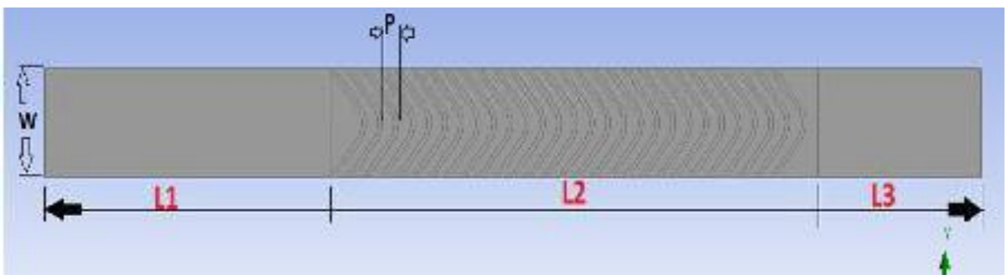

Fig. 1. V+arc roughness geometry.

Fig. 2. Multiple V+arc roughness geometry.

B. Thermo-physical properties

Air and aluminium properties are treated as constant at the average bulk temperature. The values used in the CFD model are summarized in Table 2.

Property	Air	Aluminium
Density, ρ (kg/m³)	1.225	2719
Specific heat, C_p (kJ/kg·K)	1.006	871
Viscosity, μ (N·s/m²)	1.7894×10^{-5}	—
Thermal conductivity, k (W/m·K)	0.0242	202.4
Prandtl number	0.7	—

Table 2. Thermo-physical properties used in the analysis.

C. Turbulence model and solution procedure

The airflow is assumed steady and fully turbulent. The duct walls and absorber surfaces are treated as homogeneous, with no-slip conditions at solid walls. Radiative heat transfer inside the duct is neglected. Several turbulence models were compared against the Dittus–Boelter correlation for the smooth duct. The SST k–ω model produced the closest agreement, with an average deviation of approximately 7.55%, and was therefore selected for the remaining simulations.

The continuity, momentum and energy equations are solved using a steady pressure-based formulation. The SIMPLE algorithm is used for pressure–velocity coupling and second-order upwind schemes are used for momentum and energy discretization. Residual convergence criteria are 10^{-2} for continuity, 10^{-4} for velocity components and 10^{-6} for energy. The inlet temperature is 300 K, turbulence intensity is 5%, and outlet gauge pressure is 0 N/m² with 5% backflow turbulence intensity.

D. Performance parameters

The heat-transfer coefficient is obtained from the energy balance, and the Nusselt number, Reynolds number, friction factor and thermo-hydraulic performance parameter are calculated from the relations used in the project:

$$Q = \dot{m} C_p (T_{out} - T_{in}) = h A_p (T_v - T_m)$$
$$Nu = h D_h / k$$
$$Re = \rho u L / \mu$$
$$f = 2 \Delta P D_h / (L \rho u^2)$$
$$\eta = (Nu_r/Nu_s) / (f_r/f_s)^{(1/3)}$$
$$Nu_s = 0.023 Re^{0.8} Pr^{0.4}$$
$$f_s = 0.316 Re^{-0.25}$$

E. Grid independence

A grid-independence study was performed at Re = 9000 for the smooth duct. Three meshes containing 1,687,558, 2,738,309 and 4,398,601 cells were evaluated. Ten inflation layers with a growth rate of 1.5 were applied near the walls, with the first-cell height selected to maintain $y^+ \approx 1$. The medium mesh was selected because the change in Nusselt number between the medium and fine meshes was less than 2%, while avoiding unnecessary computational cost.

Cells	Mesh size	Nu_s	ΔNu (%)	f_s	Δf (%)
1,687,558	1.75 mm	31.87	—	0.096	—
2,738,309	1.50 mm	32.03	0.50	0.094	2.08
4,398,601	1.25 mm	32.35	1.00	0.094	0

Table 3. Grid-independence test at Re = 9000.

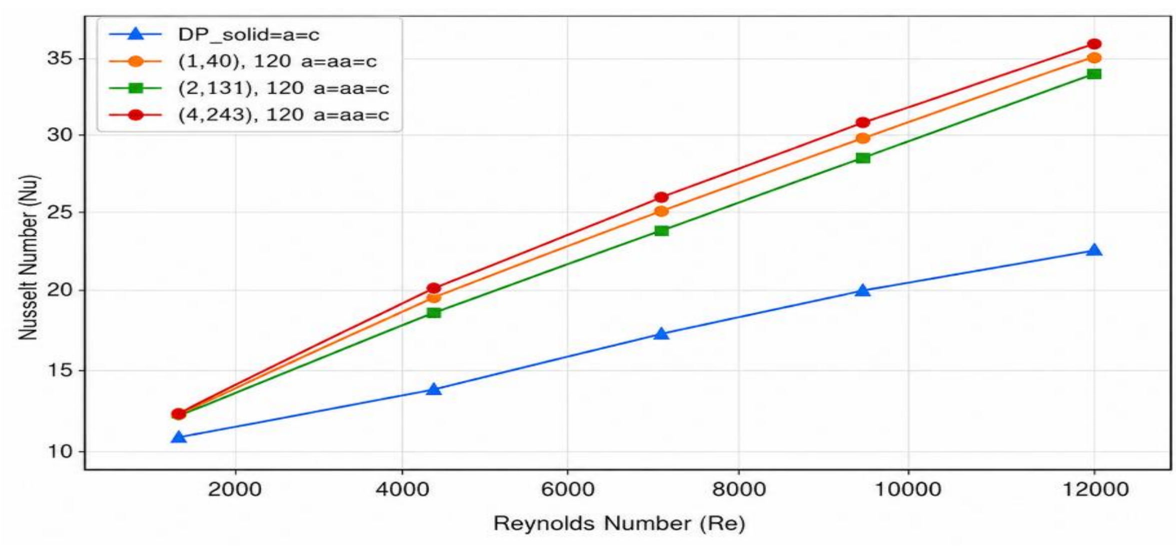

Fig. 3. Grid-independence study for the smooth absorber plate.

IV. EXPERIMENTAL METHODOLOGY

An experimental setup was fabricated to validate the computational investigation and to obtain heat-transfer, airflow and pressure-drop measurements. The test rig consists of a rectangular wooden duct, glass cover, electric lamps, centrifugal blower, flow-control valve, anemometer, PT-100 sensors, pyranometer, 16-channel data logger and U-tube manometer. The duct contains 350 mm entrance, 600 mm test and 200 mm exit sections.

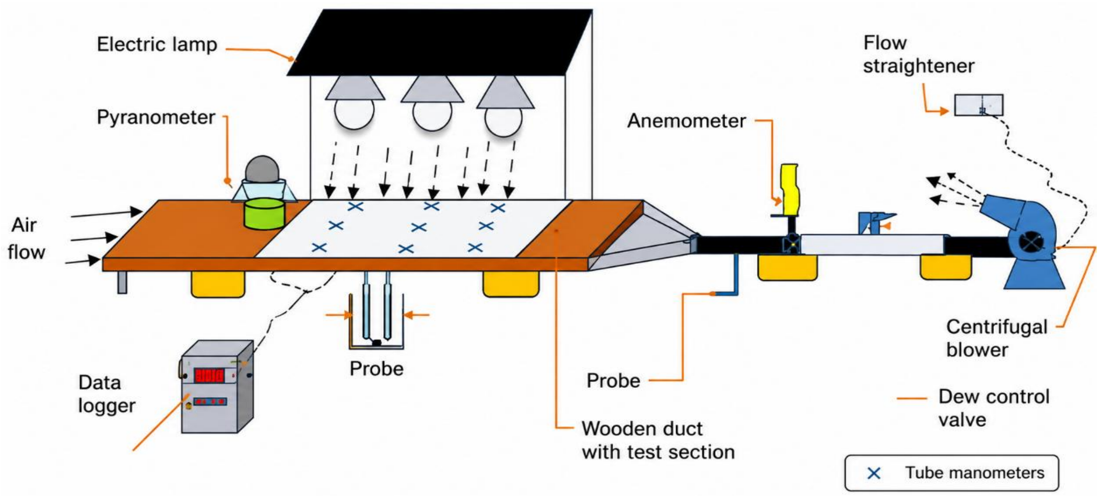

Fig. 4. Schematic diagram of the experimental setup.

The absorber plate is aluminium. Twelve 100 W filament bulbs provide a uniform heat input corresponding to 1000 W/m², monitored using a pyranometer. An 820 W centrifugal blower operating at up to 16,000 rpm draws air through the duct, while a speed regulator and flow-control valve are used to establish the desired flow condition. An anemometer measures air velocity at the outlet. Eleven PT-100 sensors are used: one probe-type sensor at the inlet, one at the outlet and nine bolt-type sensors distributed over the absorber plate. Pressure drop across the test section is measured with a U-tube manometer.

Instrument	Accuracy
PT-100 probe type	±0.1 °C
PT-100 bolt type	±0.1 °C
Anemometer	±3%
Pyranometer	1%

Table 4. Instrument accuracy.

Experiments were conducted by varying blower speed to obtain Reynolds numbers from 3000 to 11,000. Measurements were recorded after the system reached quasi-steady-state conditions. The measured quantities included absorber-plate temperature, inlet and outlet air temperature, air velocity and pressure drop. Uncertainty was evaluated using the Kline–McClintock approach described in the project.

V. RESULTS AND DISCUSSION

A. Temperature and flow fields

The temperature contours at Re = 7000 show a clear difference among the three absorber configurations. In the smooth duct, airflow remains comparatively streamlined and a thicker thermal boundary layer develops near the heated wall, producing weaker mixing and a gradual temperature rise. The V+arc configuration introduces periodic disturbances, local separation and reattachment, which improve fluid mixing and disrupt the thermal boundary layer. The Multiple V+arc arrangement produces the most complex secondary-flow structure and stronger mixing across the duct width.

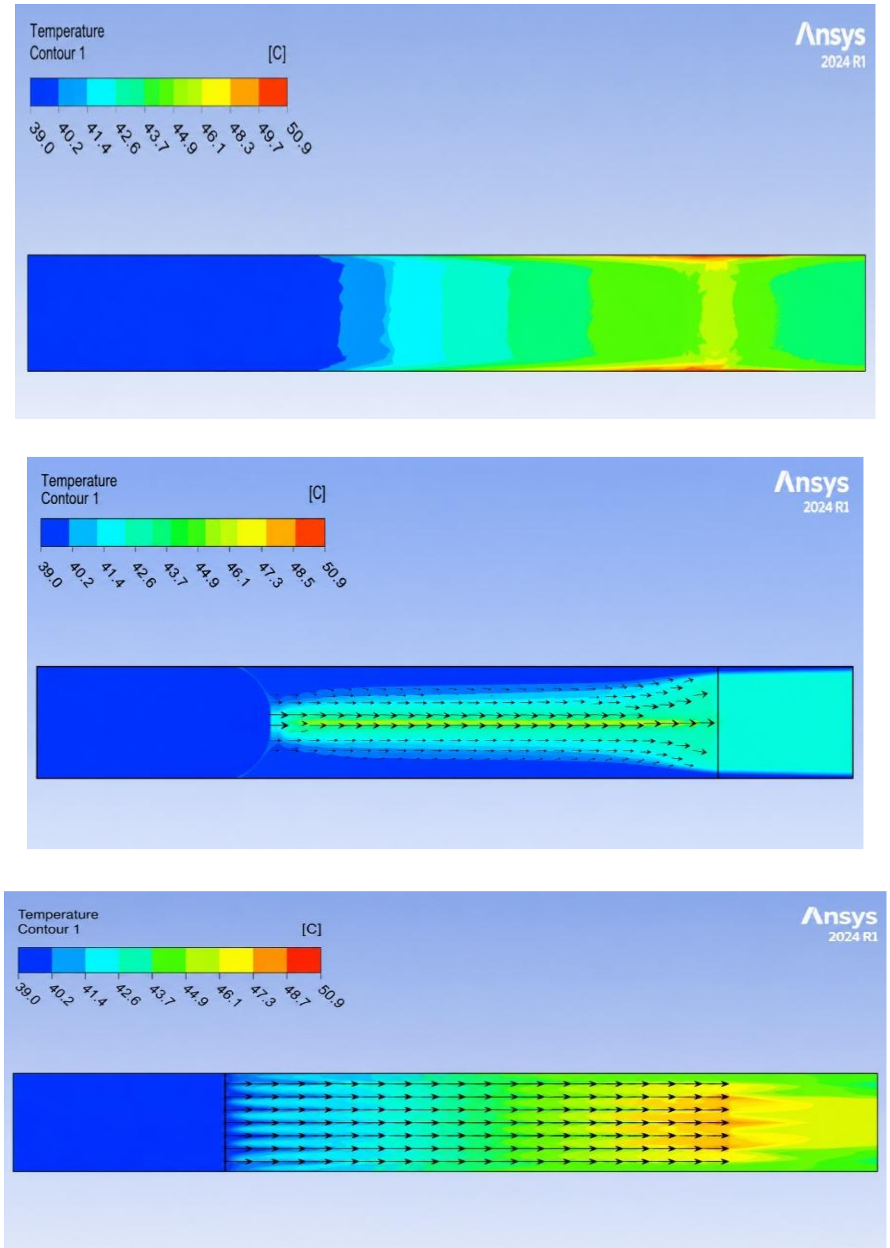

Fig. 5. Temperature contours at Re = 7000: smooth, V+arc and Multiple V+arc configurations.

The velocity contours similarly show that the smooth duct has a comparatively uniform core flow, whereas the V+arc surface creates recirculation regions downstream of the ribs. The Multiple V+arc configuration produces stronger acceleration, velocity gradients and repeated recirculation, which explains both its higher heat transfer and its higher hydraulic resistance.

© SEP 2026 | IRE Journals | Volume 10 Issue 3 | ISSN: 2456-8880
DOI: https://doi.org/10.64388/IREV10I3-1722903

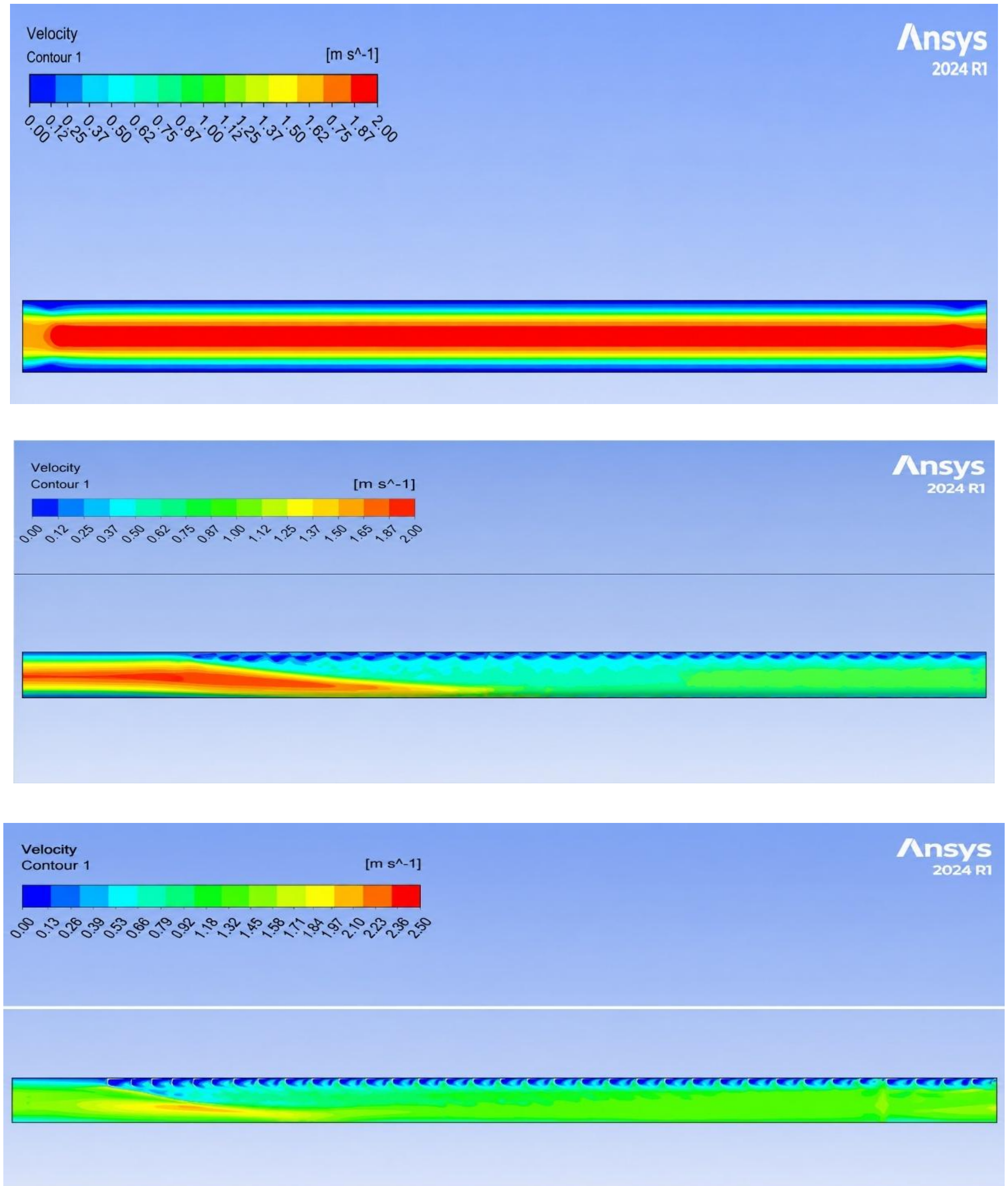

Fig. 6. Velocity contours at Re = 7000.

B. Nusselt number

Nusselt number increases with Reynolds number for all three configurations. The higher flow rate increases turbulence and reduces the effective thermal boundary-layer thickness. The smooth plate provides the lowest Nusselt number, while V+arc gives moderate enhancement. Multiple V+arc gives the highest values over the full investigated range, increasing from 37.67 at Re = 3000 to 108.93 at Re = 11,000. The project reports an enhancement of approximately 2.9–3.1 times relative to the smooth-plate baseline.

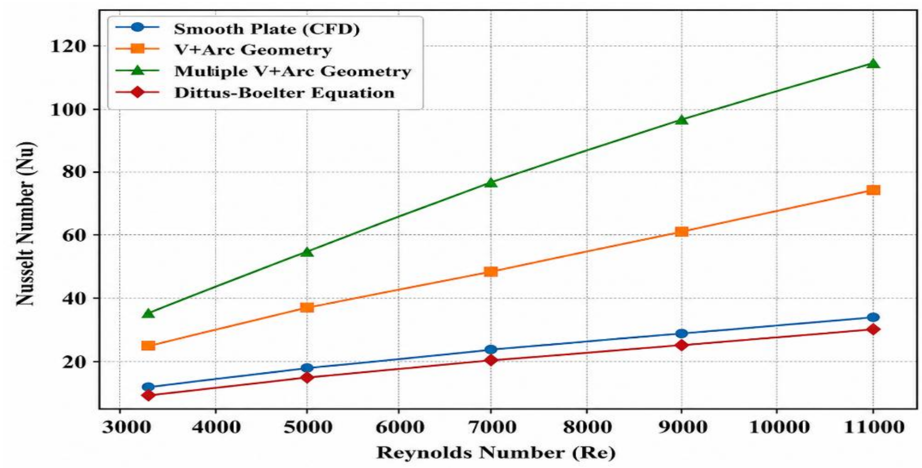

Fig. 7. Nusselt number versus Reynolds number for the investigated geometries.

Configuration	Nu range over Re = 3000–11000
Smooth plate	14.17–37.20
V+arc	24.38–72.25
Multiple V+arc	37.67–108.93

Table 5. Reported Nusselt-number ranges.

C. Pressure drop and friction factor

Artificial roughness increases pressure drop because ribs obstruct the flow and generate separation, reattachment and secondary vortices. At Re = 7000, the reported pressure drop is approximately 10.3 Pa for the smooth plate, 14.9 Pa for V+arc and 30.9 Pa for Multiple V+arc. The friction factor decreases with increasing Reynolds number, but remains higher for roughened ducts. Multiple V+arc has the highest friction factor, approximately 0.030–0.027, while V+arc ranges from about 0.017 to 0.015.

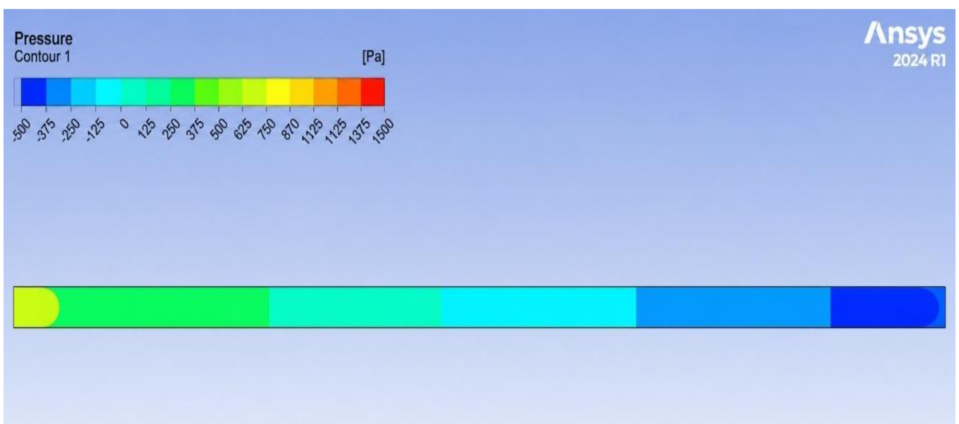

DOI: https://doi.org/10.64388/IREV10I3-1722903

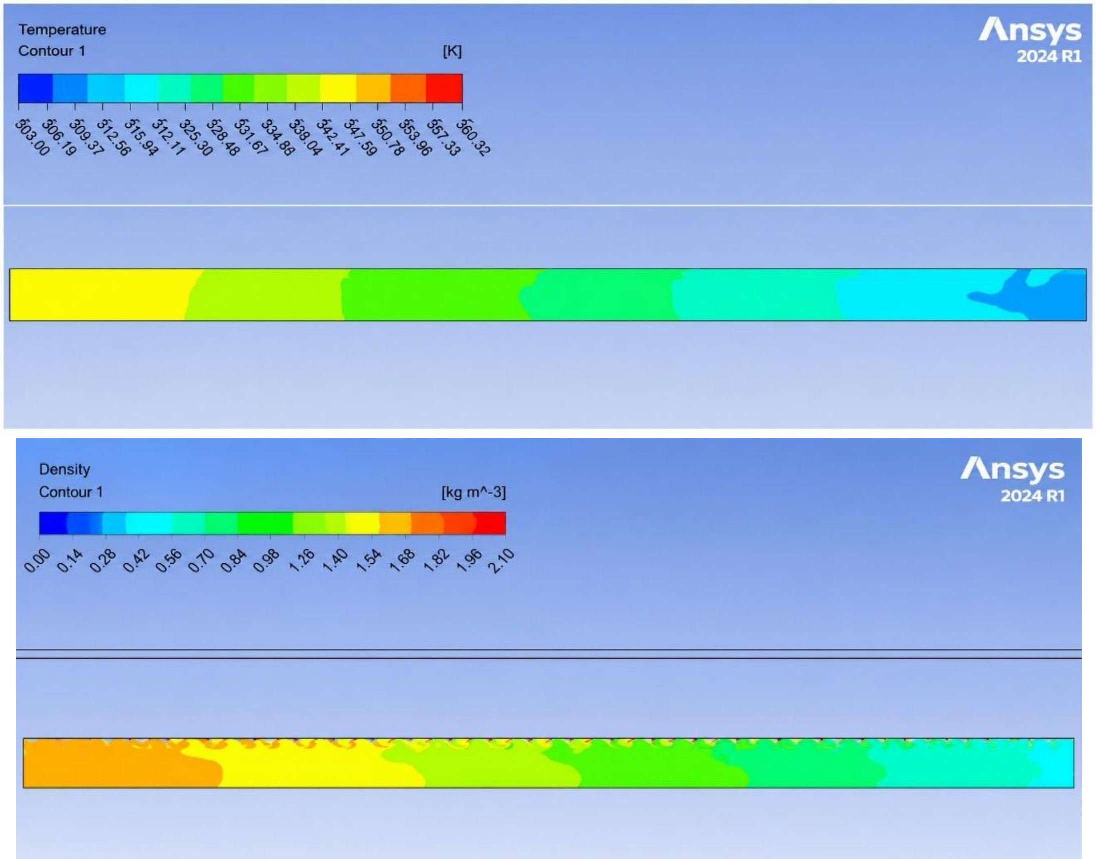

Fig. 8. Pressure contours at Re = 7000.

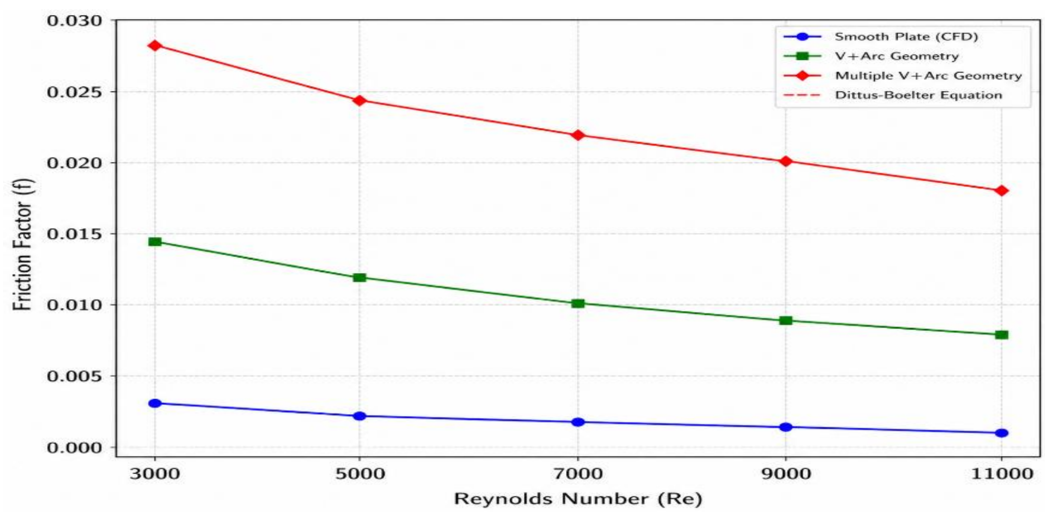

Fig. 9. Friction factor versus Reynolds number.

D. Thermo-hydraulic performance

Because heat-transfer enhancement is accompanied by an increase in pressure loss, the overall performance is assessed using the thermo-hydraulic performance parameter. Multiple V+arc consistently gives the highest reported THPP, with values from 1.99 to 2.06. V+arc gives values between 1.59 and 1.64. The maximum THPP of 2.057 is obtained at Re

= 7000, indicating that the Multiple V+arc configuration achieves a favorable balance between increased heat transfer and frictional losses at this operating condition.

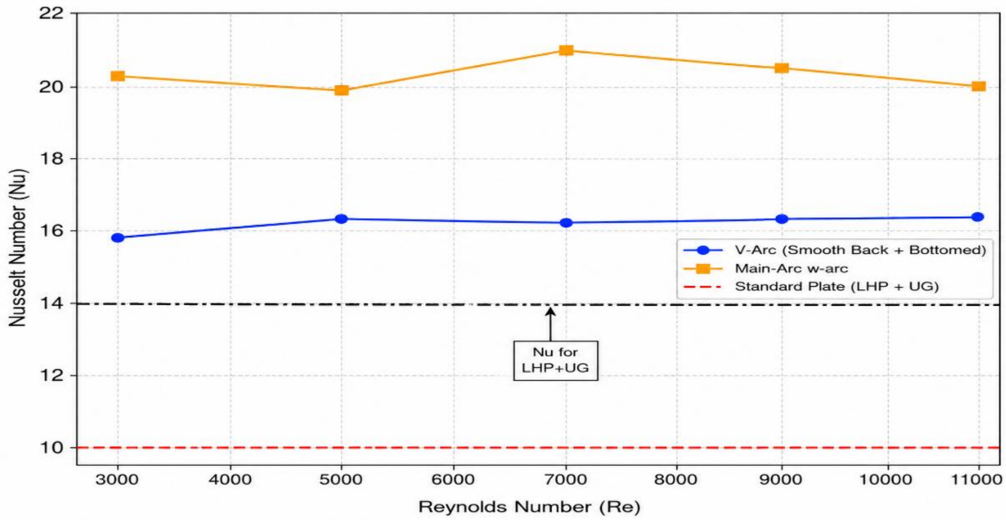

Fig. 10. Thermo-hydraulic performance parameter versus Reynolds number.

E. Experimental–CFD validation

The smooth absorber plate is used as the baseline for validating the CFD model. Experimental Nusselt-number values follow the Dittus–Boelter correlation with minimal deviation, while the friction-factor measurements agree closely with the Blasius correlation. At Re = 11,000, the project reports a smooth-plate experimental Nusselt number of 33.95 compared with approximately 37.5 from CFD. The close trend between the two datasets supports the suitability of the selected numerical approach for the subsequent roughness analysis.

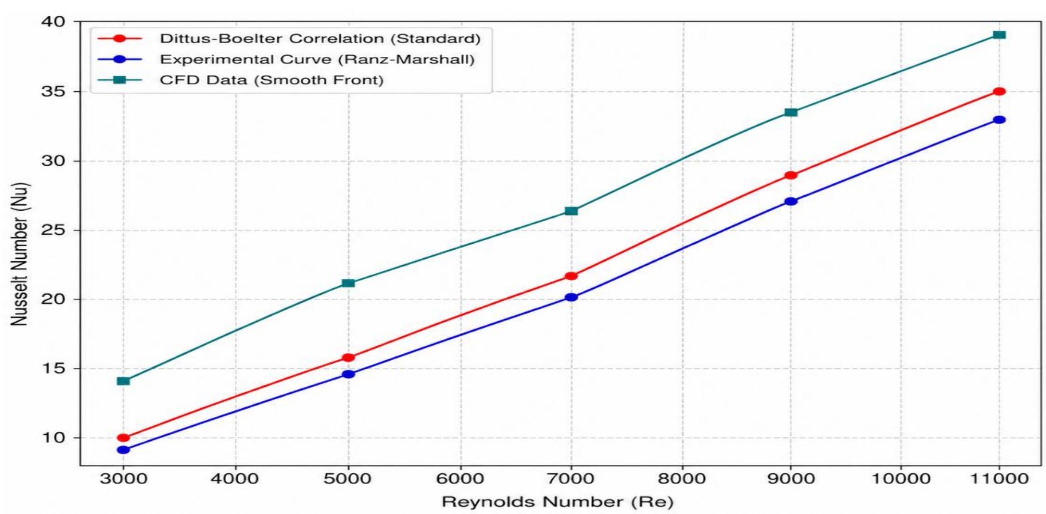

Fig. 11. Experimental and CFD comparison for the smooth plate.

VI. CONCLUSIONS AND FUTURE SCOPE

The thermo-hydraulic performance of a solar air heater equipped with V+arc and Multiple V+arc artificial roughness was investigated using CFD and experimental measurements. The main conclusions are:

- Multiple V+arc provides the strongest heat-transfer enhancement and reaches a maximum Nusselt number of 108.93 at Re = 11,000, approximately 3.1 times the smooth-plate value reported in the project.
- The improved thermal performance is associated with stronger turbulence, secondary-flow generation, boundary-layer disruption, separation and reattachment.
- Roughness increases pressure drop and friction factor. Multiple V+arc shows the largest hydraulic penalty, with friction factor approximately 0.030–0.027 over the investigated Reynolds-number range.
- The maximum thermo-hydraulic performance parameter is 2.057 at Re = 7000, indicating the best reported balance between thermal enhancement and frictional losses at this Reynolds number.
- The smooth-plate experimental results show close agreement with Dittus–Boelter and Blasius correlations, while the CFD and experimental Nusselt-number trends show good agreement.
- The study supports Multiple V+arc as a promising artificial roughness configuration for solar air heating and drying applications within the investigated operating range.

Future scope

Future work identified in the project includes varying relative roughness height and pitch, developing CFD-based correlations for Nusselt number and friction factor over a wider Reynolds-number range, and exploring the combined effect of artificial roughness with nanofluids or specialized absorber coatings.

REFERENCES

[1] S. K. Jain, G. D. Agrawal, and R. Misra, "Experimental investigation of thermohydraulic performance of the solar air heater having arc-shaped ribs with multiple gaps," *Journal of Thermal Science and Engineering Applications*, vol. 12, no. 1, 2020.

[2] Y. Mahanand and J. R. Senapati, "Thermo-hydraulic performance analysis of a solar air heater (SAH) with quarter-circular ribs on the absorber plate: A comparative study," *International Journal of Thermal Sciences*, vol. 161, 106747, 2021. Crossref

[3] S. Thakur and N. S. Thakur, "Impact of multi-staggered rib parameters of the W-shaped roughness on the performance of a solar air heater channel," *Energy Sources, Part A: Recovery, Utilization, and Environmental Effects*, pp. 1–20, 2020.

[4] A. Singh and R. Narayanan, "Advanced artificial roughness geometries for solar air heaters: A comprehensive review of wire ribs, V-shaped ribs, arc-shaped ribs, and rib-groove patterns," *Journal of Renewable Energy Research*, vol. 11, no. 4, pp. 215–229, 2025.

[5] D. S. Thakur, M. K. Khan, and M. Pathak, "Performance evaluation of solar air heater with novel hyperbolic rib geometry," *Renewable Energy*, vol. 105, pp. 786–797, 2017. Crossref

[6] A. S. Yadav and J. L. Bhagoria, "A CFD based thermo-hydraulic performance analysis of an artificially roughened solar air heater having equilateral triangular sectioned rib roughness on the absorber plate," *International Journal of Heat and Mass Transfer*, vol. 70, pp. 1016–1039, 2014. Crossref

[7] A. Kumar, R. P. Saini, and J. S. Saini, "Development of correlations for Nusselt number and friction factor for solar air heater with roughened duct having multi V-shaped with gap rib as artificial roughness," *Renewable Energy*, vol. 58, pp. 151–163, 2013. Crossref

[8] V. S. Hans, R. P. Saini, and J. S. Saini, "Heat transfer and friction factor correlations for a solar air heater duct roughened artificially with multiple V-ribs," *Solar Energy*, vol. 84, no. 6, pp. 898–911, 2010. Crossref

[9] A. Khanlari et al., "Experimental and numerical study of the effect of integrating plus-shaped perforated baffles to solar air collector in drying application," *Renewable Energy*, vol. 145, pp. 1677–1692, 2020. Crossref

[10] F. Afshari et al., "Effect of turbulator modifications on the thermal performance of cost-effective alternative solar air heater,"

Renewable Energy, vol. 158, pp. 297–310, 2020. Crossref

[11] S. V. Karmare and A. N. Tikekar, "Heat transfer and friction factor correlation for artificially roughened duct with metal grit ribs," *International Journal of Heat and Mass Transfer*, vol. 50, no. 21–22, pp. 4342–4351, 2007. Crossref

[12] S. Bhattacharyya, H. Chattopadhyay, A. Guin, and A. C. Benim, "Investigation of inclined turbulators for heat transfer enhancement in a solar air heater," *Heat Transfer Engineering*, vol. 40, no. 17–18, pp. 1451–1460, 2019.

[13] N. K. Pandey and V. K. Bajpai, "Experimental investigation of heat transfer augmentation using multiple arcs with gap on absorber plate of solar air heater," *Solar Energy*, vol. 134, pp. 314–326, 2016. Crossref

[14] V. B. Gawande, A. S. Dhoble, D. B. Zodpe, and S. Chamoli, "Experimental and CFD based thermal performance prediction of solar air heater provided with chamfered square rib as artificial roughness," *Journal of the Brazilian Society of Mechanical Sciences and Engineering*, vol. 38, no. 2, pp. 643–663, 2016. Crossref

[15] A. S. Yadav and J. L. Bhagoria, "A CFD based thermo-hydraulic performance analysis of an artificially roughened solar air heater having equilateral triangular sectioned rib roughness on the absorber plate," *International Journal of Heat and Mass Transfer*, vol. 70, pp. 1016–1039, 2014. Crossref

[16] A. E. Kabeel, M. H. Hamed, Z. M. Omara, and A. W. Kandeal, "Solar air heaters: Design configurations, improvement methods and applications – A detailed review," *Renewable and Sustainable Energy Reviews*, vol. 70, pp. 1189–1206, 2017. Crossref

[17] I. Singh and S. Singh, "A review of artificial roughness geometries employed in solar air heaters," *Renewable and Sustainable Energy Reviews*, vol. 92, pp. 405–425, 2018.

[18] T. Alam and M. H. Kim, "A critical review on artificial roughness provided in rectangular solar air heater duct," *Renewable and Sustainable Energy Reviews*, vol. 69, pp. 387–400, 2017. Crossref

[19] P. Promvonge and S. Skullong, "Heat transfer in solar receiver heat exchanger with combined punched-V-ribs and chamfer-V-grooves," *International Journal of Heat and Mass Transfer*, vol. 143, 118486, 2019. Crossref

[20] K. Nidhul et al., "Computational and experimental studies on the development of an energy-efficient drier using ribbed triangular duct solar air heater," *Solar Energy*, vol. 209, pp. 454–469, 2020. Crossref

[21] A. Singh Yadav and M. K. Thapak, "Artificially roughened solar air heater: Experimental investigations," *Renewable and Sustainable Energy Reviews*, vol. 36, pp. 370–411, 2014. Crossref

[22] A. K. Patil, J. S. Saini, and K. Kumar, "Experimental investigation of enhanced heat transfer and pressure drop in a solar air heater duct with discretized broken V-rib roughness," *Journal of Solar Energy Engineering*, vol. 137, 021013, 2015. Crossref

[23] A. Bekele, M. Mishra, and S. Dutta, "Heat transfer augmentation in solar air heater using delta-shaped obstacles mounted on the absorber plate," *International Journal of Sustainable Energy*, vol. 32, no. 1, pp. 53–69, 2013. Crossref